Multicopter Motor Damage Diagnosis Via Functionally Pooled Time Series Models: Experimental Assessment Via a Series of Flight Tests

SHINAN HUANG, JINGXI ZHU and FOTIS KOPSAFTOPOULOS

ABSTRACT

This study presents a unified statistical framework for detecting, identifying, and quantifying damage on multicopter propellers through functionally pooled (FP) time series models. Unlike conventional autoregressive models, FP models feature parameters that are explicit functions of damage magnitude, enabling parsimonious representation of damage dynamics evolution while accounting for cross-correlation between different damage states. The methodology integrates three capabilities within a single framework: health detection, motor identification, and precise damage quantification with statistical confidence intervals. Experimental validation is conducted using a hexacopter executing figure-eight flight patterns under turbulent conditions, with blade damage ranging from 2 mm to 10 mm investigated across three different rotating motors. The proposed approach achieves effective damage detection and accurate motor identification using short data segments (4 seconds) from single-channel inertial measurement unit (IMU) measurements during flight. Damage quantification is demonstrated with corresponding confidence intervals, providing statistical reliability assessment. The framework's effectiveness is evaluated through analysis of 160 s of independent test signals, demonstrating its potential for real-time fault diagnosis in autonomous aerial vehicles.

INTRODUCTION

Advanced Air Mobility (AAM), enabled by electric vertical takeoff and landing (eVTOL) technologies, is reshaping urban air transport by supporting high-frequency, on-demand services. Ensuring the safety and reliability of such operations necessitates real-time fault detection and identification (FDI) frameworks as part of autonomous health monitoring and condition-based maintenance (CBM). The importance of robust FDI systems is underscored by projected demands of 3,000–5,000 flight hours per aircraft annually [1] and a fleet size of over 37,000 vehicles by 2037 [2].

Multicopters are particularly suited for AAM due to their rotor redundancy and distributed electric propulsion. However, their complex nonlinear dynamics, strong cross-

Shinan Huang, PhD Student, Email: huangs12@rpi.edu. Intelligent Structural Systems Lab (ISSL), Department of Mechanical, Aerospace and Nuclear Engineering, Rensselaer Polytechnic Institute, Troy, NY, USA

coupling, and time-varying behavior introduce significant challenges for FDI. Existing approaches include: (i) physics-based modeling [3–5], (ii) signal processing techniques [6–10], and (iii) computational intelligence methods [11–13]. While effective in specific contexts, these methods face limitations in generalizability, robustness, and real-time scalability when addressing the complete fault diagnosis pipeline. To address these gaps, data-driven frameworks based on stochastic time series modeling have been proposed for system-level fault detection without requiring prior knowledge of system dynamics [14–16]. Recent experimental validations [17] have demonstrated their effectiveness for early-stage rotor fault diagnosis in multicopters. However, these approaches typically address individual aspects of the fault diagnosis problem—detection, localization, or quantification—rather than providing a unified solution.

In particular, real-time estimation of the propeller damage state—including detection, motor identification, and magnitude quantification—is critical for enabling damage-tolerant control, optimal trajectory planning under degraded conditions, and in-flight vehicle reconfiguration. The challenge lies in developing a methodology that can simultaneously achieve accurate fault detection, identify the specific damaged motor among multiple candidates, and provide reliable damage magnitude estimates with associated statistical confidence.

While previous investigations [18] focused on damage quantification for a single motor, the current study significantly expands the scope by presenting a unified evaluation framework that encompasses the complete fault analysis pipeline. The key contributions include: (i) development of functionally pooled autoregressive (FP-AR) models with damage-dependent parameters for parsimonious representation of multi-state dynamics, (ii) implementation of motor identification capabilities to distinguish between multiple rotating motors, and (iii) demonstration of damage quantification with statistical confidence intervals for reliability assessment. This comprehensive approach addresses the critical requirement for complete fault diagnosis in autonomous aerial systems where both accuracy and statistical reliability are essential for safe operation.

THE FLIGHTS, BLADE DAMAGE, AND DATA COLLECTION

The experimental platform consists of a custom-designed hexacopter with a total weight of approximately 8.65 kg including battery. The aircraft features a Tarot 680 Pro frame (695 mm diameter) powered by MN3110 470KV motors from T-Motor, each equipped with 300 mm diameter propellers. A 20,000 mAh battery provides sufficient power for hovering at approximately 40% throttle. Flight control is achieved through a Cube Orange Pixhawk flight controller running Ardupilot firmware, which integrates three independent IMU singals providing redundant 6-DOF measurements of linear and angular acceleration. The integrated flight controller logs all relevant signals including radio controller inputs and Electronic Speed Controller (ESC) outputs.

Controlled propeller damage is implemented by systematically trimming propeller tips in 2 mm increments, creating damage levels from 0 mm (healthy) to 10 mm, corresponding to relative damages of 0% to 3.3% with respect to the blade length (Figure 1). To evaluate motor identification capabilities, experiments are conducted on three motors sharing identical clockwise rotation direction but positioned at different locations: Motor 1 (middle), Motor 3 (front), and Motor 6 (rear), as shown in Figure 1. This config-

Figure 1. (Left) The Hexacopter used for data collection. (Middle) Healthy and damaged propellers with tips clipped off by $2 \sim 10$ mm with 2 mm increment. (Right) Waypoints are designed to approximate an 8-pattern flight path.

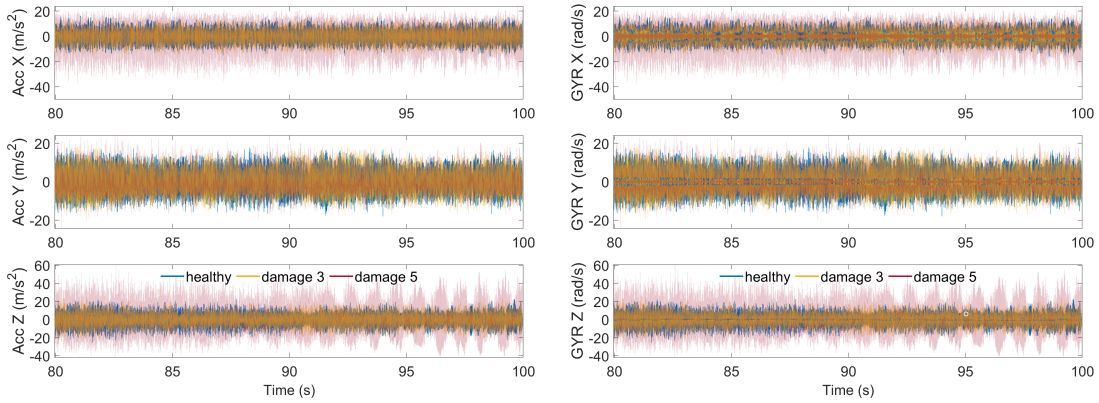

Figure 2. Comparison of linear acceleration (left) and gyroscpoe (right) IMU signals for three damage states: healthy, damage 3 (6 mm), and damage 5 (10 mm).

uration enables assessment of the framework's ability to distinguish between identically operating motors under various damage conditions. Data collection is performed during low-altitude figure-eight flight patterns executed under challenging outdoor conditions with peak wind speeds of 12 m/s and average speeds of 5 m/s. The flight trajectory is programmed using waypoints in the mission planner to approximate the desired pattern (Figure 1). Each experimental trial consists of two complete laps followed by landing, with total flight duration of 300 s including takeoff and landing phases.

The experimental protocol tests each of the three selected motors across all damage levels, ensuring consistent flight conditions and data collection procedures. Linear acceleration and gyroscope data are acquired from the IMU at 1000 Hz sampling rate, while altitude measurements are obtained from the integrated barometer. Figure 2 demonstrates the collected signals between healthy conditions and two representative damage states (6 mm and 10 mm) for both acceleration and gyroscope measurements.

The collected dataset provides coverage of multicopter dynamics under varying damage conditions and environmental disturbances. The turbulent flight conditions serve as a realistic testing scenario that challenges the robustness of the proposed FP-AR framework. Signal analysis reveals distinct spectral characteristics associated with different damage levels and motor locations, providing the foundation for the subsequent parametric identification and statistical analysis procedures detailed in the following sections.

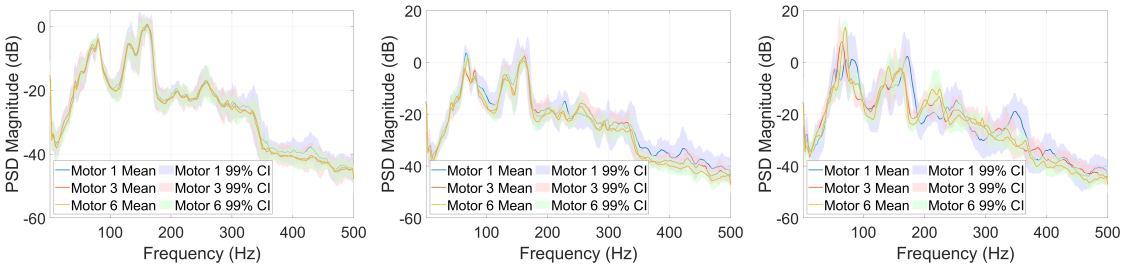

Figure 3. Comparison of x-Linear acceleration PSD for three motors under three damage states including healthy, damage 3 (6 mm) and damage 5 (10 mm). The 99% confidence intervals of the estimated Welch-PSD are shown for the healthy case as shaded areas.

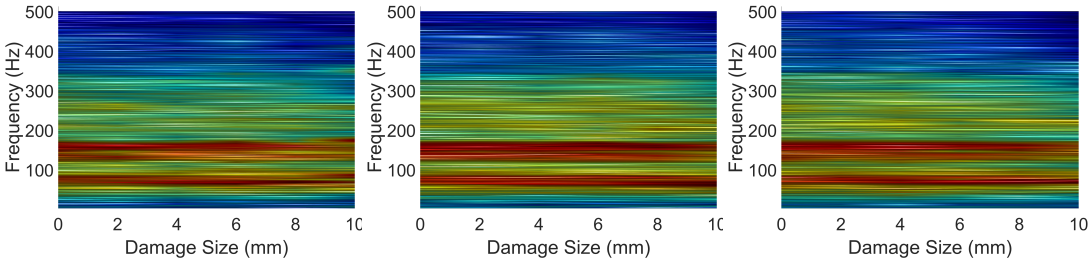

Figure 4. Non-parametric damage topology model based PSD magnitude versus frequency for Motors 1 (Left), 3 (Middle), and 6 (Right).

STOCHASTIC MODELING UNDER MULTIPLE DAMAGE STATES

Non-parametric analysis provides an initial assessment of how propeller damage affects aircraft dynamics without assuming specific model structures. This approach serves as both a validation tool for damage detectability and a foundation for subsequent parametric model development. The analysis focuses on Power Spectral Density (PSD) estimation using Welch's method [19] to reveal frequency-domain characteristics that distinguish between healthy and damaged states.

Figure 3 presents comparative PSD analysis for x-direction linear acceleration across the three motors under three damage states: healthy (left), 6 mm damage (center), and 10 mm (right) damage. The analysis employs 250-second signal segments (sampling frequency Fs = 1000 Hz; window of 1024 samples, 50% overlap, 1024-point FFT, Matlab function pwelch.m). To quantify statistical significance, signals are divided into 25 equal segments, enabling calculation of mean and standard deviation for the healthy baseline state with 99% confidence intervals shown as shaded regions. The spectral analysis reveals distinct frequency-dependent signatures associated with different damage levels. As damage increases, characteristic shifts in spectral content become evident, particularly in frequency ranges corresponding to rotor harmonics and structural response modes. These changes reflect the altered aerodynamic and dynamic characteristics of damaged propellers, providing initial evidence that damage detection for higher magnitude levels is feasible through frequency-domain analysis.

Figure 4 presents non-parametric damage topology models that capture the relationship between damage magnitude and frequency for each motor. These topology models

demonstrate how spectral content evolves continuously as a function of damage size, revealing motor-specific damage signatures that enable both damage detection and motor identification. The non-parametric results establish three key findings: (i) for larger damage spectral changes are statistically significant and exceed baseline confidence intervals, (ii) each motor exhibits distinct spectral signatures that facilitate identification, and (iii) damage magnitude correlates with systematic spectral variations.

Parametric Identification

While non-parametric analysis confirms damage detectability and provides valuable insights into spectral characteristics, it lacks the precision and parsimony required for quantitative damage assessment. Traditional autoregressive (AR) models require separate identification for each operating condition, leading to multiple independent models that cannot capture the systematic evolution of dynamics across damage states. In contrast, Functionally Pooled AutoRegressive (FP-AR) models embed the damage parameter directly into the model structure, creating a single unified model that represents the entire damage evolution continuum. The key innovation of FP-AR models lies in expressing the AR parameters as explicit functions of the damage magnitude, rather than treating them as independent parameters. This approach offers three critical advantages: (i) parsimony, i.e., a single model captures all damage states rather than requiring multiple separate models, (ii) continuity, as the model can predict dynamics for any damage level within the training range, including untested intermediate values, and (iii) statistical efficiency as the approach leverages cross-correlation between different damage states, improving parameter estimation accuracy compared to individual models.

The univariate Functional Principal AutoRegressive (FP-AR)$(na)_{pa}$ model for a given damage state k is defined as:

$$y_k[t] = \sum_{i=1}^{na} a_i(k) \cdot y_k[t-i] + e_k[t], \quad e_k[t] \sim \mathcal{N}(0, \sigma_e^2(k)) \tag{1}$$

where the autoregressive parameters $a_i(k)$ vary with damage state k and are modeled as projections onto a low-dimensional functional subspace defined by basis functions. These coefficients are estimated across all damage cases simultaneously by expressing the time series data in a global linear-in-parameters form that combines lagged values with basis function evaluations. The global parameter vector is estimated using Weighted Least Squares (WLS) to account for potentially heteroscedastic residuals across damage states. Model structure selection—specifically the AR order (na) and functional subspace dimensionality (pa)—is achieved using the Bayesian Information Criterion (BIC) to balance model fit with parsimony. For a detailed mathematical derivation and implementation see [20].

FP-AR models are constructed individually for each motor using 4-second data segments (4000 samples) extracted from the flights. The selected FP-AR models configurations are: FP-AR$(33)_5$ for Motor 1, FP-AR$(35)_2$ for Motor 3, and FP-AR$(36)_4$ for Motor 6. Figure 5 presents the parametric damage topology models, showing spectral magnitude as function of both frequency and damage size for each motor. Compared to the non-parametric results (Figure 4), the FP-AR models provide significantly cleaner representation with reduced noise, offering more detailed and reliable information about

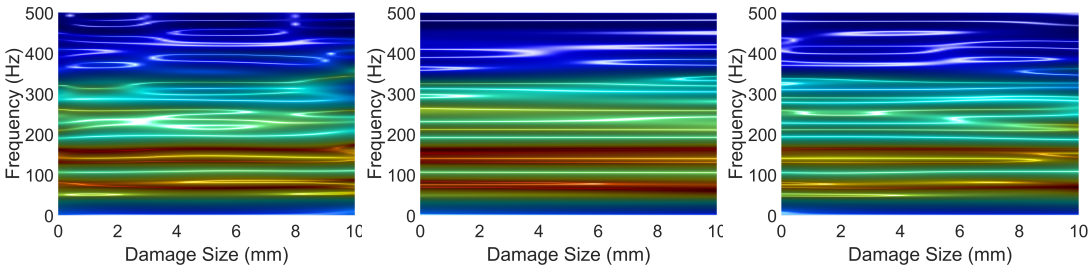

Figure 5. Parametric damage topology model based PSD magnitude versus frequency for Motors 1 (Left), 3 (Middle), and 6 (Right).

damage-dependent spectral evolution. The superior performance of FP-AR models over non-parametric approaches is evident in the reduced noise and enhanced detail visible in Figure 5. The models successfully capture the systematic evolution of spectral characteristics as damage progresses, providing the foundation for quantitative damage assessment. The ability to represent damage dynamics as continuous functions rather than discrete states enables more precise damage quantification and supports the development of confidence intervals for statistical reliability assessment, as demonstrated in the subsequent analysis sections.

DAMAGE DETECTION, IDENTIFICATION AND QUANTIFICATION

The trained FP-AR models enable a three-stage fault diagnosis framework: damage detection (determining if damage exists), motor identification (localizing damage to specific motors), and damage quantification (estimating magnitude with confidence bounds). Damage detection is formulated as a statistical hypothesis test where the damage magnitude k serves as the decision parameter. Given an unknown signal, the FP-AR model is re-parameterized to estimate k by minimizing prediction error. The model for the unknown state is written as:

$$M_V(k, \sigma_e^2(k)) : y_u[t] = \sum_{i=1}^{na} a_i(k) \cdot y_u[t-i] + e_u[t, k] \tag{2}$$

The damage magnitude $\hat{k}$ and the associated residual variance are estimated by minimizing the prediction error of the FP-AR model, treated as a function of the unknown parameter k. This optimization is typically solved using gradient-based methods (see [20, 21] for the full formulation).

Under the healthy assumption $(k = 0)$, the estimator $\widehat{k}$ follows an asymptotically Gaussian distribution $\hat{k} \sim \mathcal{N}(k, \sigma_k^2)$, enabling construction of a t-statistic for hypothesis testing. The decision framework compares the computed t-statistic against critical values at specified confidence levels enabling damage detection with quantified false alarm rates [20]. Damage detection is then framed as the following hypothesis test:

$$H_o : k = 0 \quad \text{(healthy motor)}, \qquad H_1 : k \neq 0 \quad \text{(damaged motor)} \tag{3}$$

Under H_o, the test statistic follows t-distribution , $t = \frac{\hat{k}}{\hat{\sigma}_k} \sim t(N-1)$ [20].

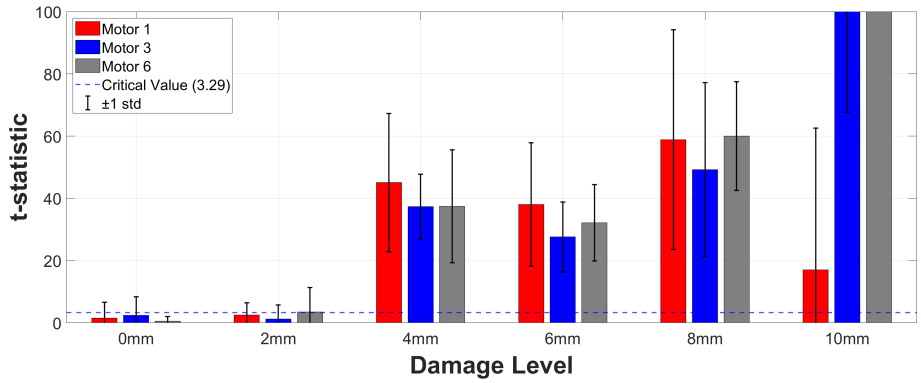

Figure 6. Damage detection results for three motors: t-statistic (bars) and the critical points (- - -) at the $\alpha = 0.001$ risk level. Bars represent the mean t-statistic over 41 test sets (from 30–190 s), with error bars denoting ± 1 std. Damage is detected if t exceeds the critical point.

Figure 6 demonstrates indicative damage detection results via AccX signals across three motors using 41 independent test segments. The framework successfully distinguishes damaged conditions (4-10 mm) from healthy states, with t-statistics consistently exceeding critical thresholds. For smaller damage levels (2 mm), detection becomes more challenging but remains statistically significant in most cases. This performance characteristic is crucial for early-stage damage detection in operational scenarios where timely intervention prevents catastrophic failure.

Motor identification determines which motor model best represents the current system dynamics by applying test data to all candidate FP-AR models and evaluating residual characteristics. The approach employs whiteness testing of normalized residual autocorrelation using a Q-statistic with χ^2 distribution properties. The model producing residuals closest to white noise is identified as the correct damage topology. Validation is based on hypothesis testing of the normalized residual autocorrelation [20]:

$$\begin{aligned} H_0 &: \rho_V[\tau] = 0 \quad \text{for all } \tau = 1, \ldots, r \qquad \text{(motor model } V \text{ is valid)} \\ H_1 &: \rho_V[\tau] \neq 0 \quad \text{for some } \tau \qquad\quad \text{(motor model } V \text{ is invalid)} \end{aligned} \tag{4}$$

The test statistic used is the Q-statistic, $Q = N(N+2)\sum_{\tau=1}^{r} \frac{1}{N-\tau}\hat{\rho}_V[\tau]^2 \sim \chi^2(r)$ [20], where $\hat{\rho}_V[\tau]$ denotes the estimated residual autocorrelation at lag τ, N is the residual sequence length, and r the number of lags. The model corresponding to the accepted hypothesis is identified as the one most consistent with the damaged motor dynamics.

Figure 7 shows indicative motor identification results based on AccX signals where Motor 6 consistently produces the lowest Q-statistic, remaining below critical thresholds across damage levels. For each test segment, the Q-statistic was calculated based on $N = 400$ residual samples and lag parameter $r = 20$. The mean and standard deviation of the resulting Q-statistics were computed, as shown in Figure.7 The statistical confidence provided by the Q-test ensures reliable motor identification even under varying flight conditions and environmental disturbances.

Damage magnitude estimation provides interval estimates with associated confidence bounds obtained from the corresponding re-parameterized FP-AR model (corresponding to the damaged motor). The framework computes damage estimates $\widehat{k}$,

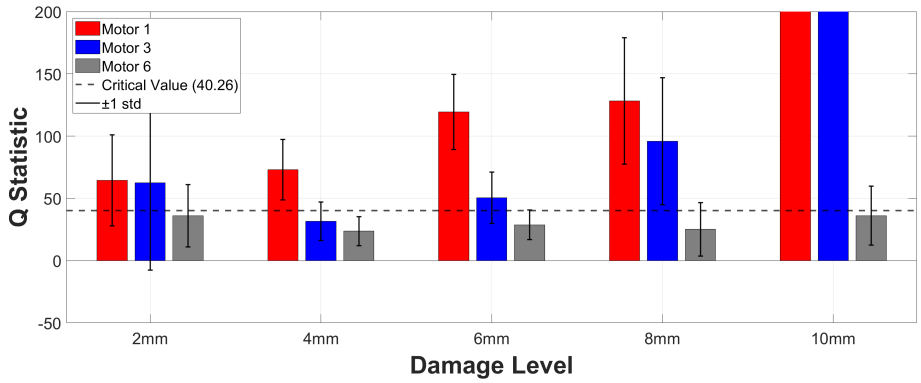

Figure 7. Motor 6 identification results with Q-statistics computed from 21 test sets (sampled between 58 and 138 seconds). Bars represent the mean Q-statistic for each candidate motor model (Motor 1, 3, and 6), with error bars indicating ± 1 standard deviation. The dashed line shows the critical value at the $\alpha = 0.1$ risk level. For each damage level, the corresponding damage topology (motor model) is accepted as valid if its Q-statistic lies below the critical threshold.

and associated variances $\widehat{\sigma}_k^2$, enabling construction of confidence intervals at specified Type I risk levels (α), $\left[\hat{k} + t_{\frac{\alpha}{2}}(N-1)\hat{\sigma}_k, \quad \hat{k} + t_{1-\frac{\alpha}{2}}(N-1)\hat{\sigma}_k\right]$ where t_α designates the distribution t (with the indicated degrees of freedom) α critical point (defined as $\mathbb{P}[t \leq t_\alpha] = \alpha$) and $\widehat{\sigma}_k$ is the positive square root of the variance obtained $\widehat{\sigma}_k^2$.

Figure 8 presents indicative damage quantification results using the AccX signals across 21 independent test segments extracted between 74 to 78 seconds, showing estimated damage ranges (mean $\pm$ standard deviation) compared to true damage levels. For each damage level, the mean residual sum of squares (RSS) was calculated and the estimated damage range was determined by plotting the mean $\pm$ standard deviation (blue dashed lines). The framework demonstrates increasing accuracy with damage magnitude, reflecting improved signal-to-noise ratio for larger damage states. The confidence intervals provide essential uncertainty bounds that enable risk-based decision making in operational scenarios.

CONCLUDING REMARKS

This study presented a unified statistical framework for multicopter propeller fault diagnosis based on functionally pooled autoregressive (FP-AR) models. The approach integrates damage detection, motor identification, and damage quantification within a single methodology, addressing the complete fault diagnosis pipeline required for autonomous aerial systems.

The main findings from this investigation are: (1) Non-parametric analysis confirms that PSD estimates provide clear evidence of changing aircraft dynamics for larger damage magnitudes, establishing the foundation for more sophisticated parametric modeling approaches. (2) FP-AR models successfully achieve damage detection, damaged motor identification, and damage magnitude estimation under realistic flight conditions, with statistical confidence levels providing reliability assessment for each diagnosis stage. (3) Robustness under control compensation is demonstrated as the method distinguishes

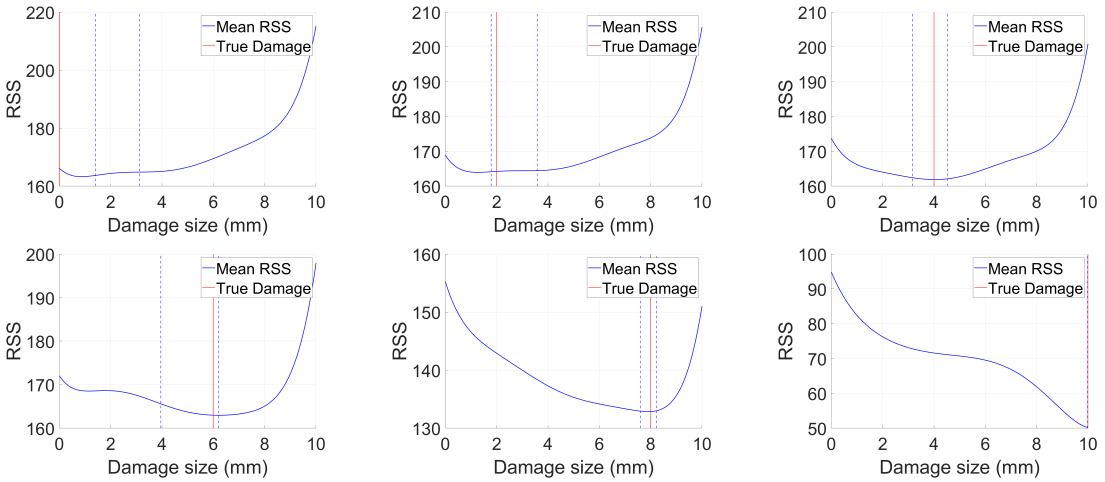

Figure 8. Indicative Motor 6 damage magnitude estimation results based on the Residual Sum of Squares (RSS) loss function across different damage levels (healthy to 10 mm). Each subplot corresponds to a specific true damage level (0 mm, 2 mm, 4 mm, 6 mm, 8 mm, and 10 mm; left to right, top to bottom). The blue curve represents the mean RSS over 21 test segments (58–138 s), while the red vertical line indicates the true damage level. The blue dashed lines denote the estimated damage mean $\pm$1std across test sets.

faulty from healthy states even when flight controllers compensate for damage effects and return the aircraft to steady flight. (4) Sensor agnostic methodology enables application to various sensor types (acceleration, rate gyros, strain gauges), providing flexibility for different aircraft configurations and monitoring requirements. The framework demonstrated potential for real-time fault diagnosis using short data segments (4 seconds) from standard onboard sensors. The statistical foundation provides quantified uncertainty bounds essential for safety-critical decision making in autonomous operations.

REFERENCES

1. 2016. “Fast-Forwarding to a Future of On-Demand Urban Air Transportation,” Tech. rep.
2. 2019, “Automation vs. Autonomy in Urban Air Mobility,” [Online; accessed 3-September-2020].
3. 2002. “System Identification Modeling of a Small-Scale Unmanned Rotorcraft for Flight Control Design,” 47(1):50–63, doi:/10.4050/JAHS.47.50.
4. Freddi, A., S. Longhi, A. Monteriù, and M. Prist. 2014. “Actuator Fault Detection and Isolation System for an Hexacopter,” in *IEEE/ASME 10th International Conference on Mechatronic and Embedded Systems and Applications*, IEEE/ASME, doi: 10.1109/MESA.2014.6935563.
5. Serafini, J., G. Bernardini, R. Porcelli, and P. Masarati. 2019. “In-flight health monitoring of helicopter blades via differential analysis,” *Aerospace Science and Technology*, 88:436–443, ISSN 1270-9638, doi:https://doi.org/10.1016/j.ast.2019.03.039.
6. Waschburger, R., H. M. Paiva, J. J. R. e Silva, and R. K. H. Galvão. 2010. “Fault detection in a laboratory helicopter employing a wavelet-based analytical redundancy approach,” in *Conference on Control and Fault-Tolerant Systems, Nice, France*, pp. 70–75.
7. Schwartz, B. C. and D. L. Jones. 2000. “Quadratic and instantaneous frequency analysis of helicopter gearbox faults,” *Mechanical Systems and Signal Processing*, 14(4):579–595.

8. Cox, J. R., S. Arnold, and P. Anusonti-Inthra. 2016. “Rotor Blade Fault Detection through Statistical Analysis of Stationary Component Vibration,” in *52nd AIAA/SAE/ASEE Joint Propulsion Conference*, doi:10.2514/6.2016-4642.
9. Lu, F., Z. Li, J. Huang, and M. Jia. 2020. “Hybrid State Estimation for Aircraft Engine Anomaly Detection and Fault Accommodation,” *AIAA Journal*, 58(4):1748–1762, doi:10.2514/1.J059044.
10. Rao, M. E., J. Simon, J. Moll, and M.-F. Schütz. 0. “Real-time onboard propeller fault diagnosis of autonomous delivery drones through vibration analysis,” *Structural Health Monitoring*, 0(0):14759217251327224, doi:10.1177/14759217251327224.
11. Zhao, X. and L. Chen. 2022. “Prediction of Rotor Loads Using Neural Networks for Health Monitoring of Composite Rotor Blades,” *Aerospace Science and Technology*, 126:107618, doi:10.1016/j.ast.2022.107618.
12. Smith, J. and Y. Wang. 2021. “Fault-Tolerant Trajectory Control Using Adaptive Neural Networks for Multirotor UAVs,” in *2021 IEEE International Conference on Robotics and Automation (ICRA)*, pp. 1724–1730, doi:10.1109/ICRA2021.9475678.
13. Garcia, M. and P. Torres. 2023. “Probabilistic Machine Learning for Fault Diagnosis in Multirotor UAVs Under Dynamic Conditions,” in *2023 AIAA/IEEE Digital Avionics Systems Conference (DASC)*, pp. 1452–1458, doi:10.1109/DASC2023.1123456.
14. Dutta, A., M. McKay, F. Kopsaftopoulos, and F. Gandhi. 2021. “Statistical residual-based time series methods for multicopter fault detection and identification,” *Aerospace Science and Technology*, 112:106649, ISSN 1270-9638, doi:https://doi.org/10.1016/j.ast.2021.106649.
15. Dutta, A., M. McKay, F. Kopsaftopoulos, and F. Gandhi. 2020. “Rotor Fault Detection and Identification on a Hexacopter under Varying Flight States Based on Global Stochastic Models,” in *Vertical Flight Society 76th Annual Forum, Online (due to COVID-19)*, AHS.
16. Dutta, A., M. E. McKay, F. Kopsaftopoulos, and F. Gandhi. 2022. “Multicopter Fault Detection and Identification via Data-Driven Statistical Learning Methods,” *AIAA Journal*, 60(1):1–16, doi:10.2514/1.J060353.
17. Huang, S., J. Zhu, P. Zhou, C. Vining, and F. P. Kopsaftopoulos. 2024. “Data-Driven Probabilistic Health Monitoring on a Hexacopter via Time-Series Assisted Machine Learning Methods,” *Proceedings of the Vertical Flight Society 80th Annual Forum*.
18. Huang, S., J. Zhu, P. Zhou, and F. Kopsaftopoulos. “A Functional Time Series Framework for Probabilistic Health Monitoring on a Hexacopter: Experimental Evaluation via a Series of Flight Tests,” in *AIAA SCITECH 2025 Forum*, doi:10.2514/6.2025-2671.
19. Ljung, L. 1999. *System Identification: Theory for the User*, Prentice–Hall, 2nd edn.
20. Kopsaftopoulos, F. P. and S. D. Fassois. 2013. “A functional model based statistical time series method forvibration based damage detection, localization, andmagnitude estimation,” *Mechanical Systems and Signal Processing*, 39:143–161.
21. Dutta, A., R. Niemiec, F. Kopsaftopoulos, and F. Gandhi. 2021. “Unified Statistical Framework for Rotor Fault Diagnosis on a Hexacopter via Functionally Pooled Stochastic Models,” in *Proceedings of the 77th Annual Forum*, The Vertical Flight Society, Virtual.